

Spatiotemporal Chaos and Noise

Gottfried Mayer-Kress¹ and Kunihiko Kaneko²

Received June 25, 1988; revision received July 30, 1988

Low-dimensional chaotic dynamical systems can exhibit many characteristic properties of stochastic systems, such as broad Fourier spectra. They are distinguishable from stochastic processes through finite values for their dimension, Lyapunov exponents, and Kolmogorov-Sinai entropy. We discuss how these characteristic observables are modified in spatiotemporal chaotic systems like coupled map lattices. We analyze with the help of Lyapunov concepts how the stochastic limit is approached and how these properties can be observed directly through local dimension measurements from reconstructed time series. Finally, we discuss the interaction of spatiotemporal attractors with external noise and possible connections to problems of pattern selection and stability.

KEY WORDS: Fractal dimensions; Lyapunov spectra; comoving Lyapunov dimension; coupled map lattice; spatiotemporal chaos; noise-induced transitions.

1. INTRODUCTION

The study of chaotic dynamics has given us a new perspective on erratic phenomena in nature. It is well known that erratic behavior can originate from deterministic mechanisms.⁽¹⁾

How can deterministic chaos be distinguished from random noise? Let us first recall some properties of random processes: According to Chaitin⁽²⁾ and Kolmogoroff,⁽³⁾ randomness is defined as the incompressibility of data in the sense that there exists no deterministic process which can reproduce the data and which uses less information than is needed to just copy the

¹ Santa Fe Institute, Santa Fe, New Mexico 87501, and Center for Nonlinear Studies, Los Alamos National Laboratory, Los Alamos, New Mexico 87545.

² Institute of Physics, College of Arts and Sciences, University of Tokyo, Komaba, Meguro-ku, Tokyo 153, Japan, and Center for Complex Systems Research, University of Illinois at Urbana-Champaign, Champaign, Illinois 61820.

data. It is shown, however, by Chaitin⁽²⁾ with the use of Gödel's theorem that we cannot prove that any given time series is "random" in that sense.

On the other hand, the converse procedure (i.e., to determine that a given time series is not random in the sense of algorithmic complexity) can be carried out in some cases. Most of the modern methods for this procedure are based on geometrical reconstruction of the dynamics in state spaces with increasing dimensionality.^(4,5) An overview of methods for estimating the minimal dimensionality of a state space which contains all the relevant dynamics can be found in refs. 6 and 7.

Although these procedures have been successful in the past, an important constraint lies in the fact that they are based on the assumption of the existence of a low-dimensional attractor ($D < 10$, say). The assumption seems to hold in cases like the onset of turbulent time dependence of the fluid motion in cells of small aspect ratio in Benard or Taylor experiments.

It is different, however, in the case of turbulence or spatiotemporal chaos. If the spatial correlations decay at length scales smaller than the system size, the dimension is assumed to be proportional to the system size and thus rather large in most experimental systems. A motivation for the present paper is to search for algorithms which allow one to distinguish spatiotemporal chaos from random processes.

Under "spatiotemporal chaos" we understand a deterministic dynamical system which shows temporal chaos at each lattice site and which has a nontrivial incoherent structure in space. It can serve as model for fluid turbulence, chemical reaction systems, plasmas, liquid crystals, solid-state systems (charge density waves, Josephson junction arrays, spin waves), and perhaps also biological information processing networks. A simple and essential model for spatiotemporal chaos, which we want to use in this paper, consists of local iterated maps on a lattice with diffusive coupling.⁽⁸⁻¹⁷⁾

A coupled map lattice (CML) is a dynamical system with discrete time, discrete space, and continuous state as well as continuous control parameters (refs. 8, 9, 18, and 19; see also refs. 20-24). This combination of discrete and continuous variables is optimal for numerical simulations in which only moderate spatial and temporal accuracy is required but where we are interested in identifying bifurcations for which it is necessary to have precise control over the state and parameters.

In this paper, we restrict ourselves to the following nonlinear local dynamics with diffusive coupling:

$$x_{n+1}(i) = (1 - \mu) f(x_n(i)) + \frac{1}{2}\mu[f(x_n(i+1)) + f(x_n(i-1))] + \xi_n(i) \quad (1)$$

where $x_n(i)$ is the scalar state variable at a discrete time n and lattice point

$i(i=1, 2, \dots, N = \text{system size})$ with periodic boundary conditions. Here the mapping function $f(x)$ is chosen to be the logistic map

$$f(x) = 1 - ax^2 \quad (2)$$

and $\xi_n(i)$ is assumed to be a random perturbation, δ -correlated both in space and time.

We show that in a dimensional context the coupled map lattice indeed acts like a noise source in that dimensions measured from a local time series do not converge to a finite value as the embedding dimension is increased. We confirm this through direct embedding and dimension estimations as well as through estimation of Lyapunov exponents. In the case of one-dimensional lattices we observe that the rate of increase of the dimensional complexity is significantly smaller than for comparable white noise (simulated with a standard random number generator). For planar lattices, however, the Lyapunov dimension depends quadratically on the embedding dimension, i.e., beyond a critical embedding dimension we cannot discriminate the signal produced by the two-dimensional lattice from stochastic white noise. This is qualitatively different from results for coupled chains of maps.

In the last section we present some results on the same system of coupled maps with parameters for which we observe stable regions of periodic behavior interrupted by patches of chaotic oscillations. We show evidence that these patterns are attractors in the sense that they are stable against low-level noise. Their relative stability (in the absence of any Lyapunov functional) can be estimated by their robustness against external noise.

2. GEOMETRICAL RECONSTRUCTION AND CORRELATION DIMENSION

Let us briefly review the reconstruction and estimate of dimension. First, take an embedding dimension k and reconstruct the phase space following the method of Packard *et al.*⁽⁴⁾ and Takens.⁽⁵⁾ To this end, we consider a scalar time series x_m and define the k -dimensional vector time series

$$\mathbf{x}_m = (x_m, x_{m-\tau}, \dots, x_{m-(k-1)\tau}) \quad (3)$$

where $\tau > 0$ is a fixed time delay. For the estimation of the dimension we apply a slight modification of a method introduced by Grassberger and Procaccia.^(25,26) Consider the number $n_k(r)$ of pairs of vectors $\mathbf{x}_m, \mathbf{x}_l$ which are separated by a distance (in the k -dimensional space) less than r . The

dimension D_k of the reconstructed data set in k space and its dynamical entropy K_k can be defined by

$$\eta_k(r) = \gamma r^{D_k} e^{k\tau K_k} \quad (4)$$

where γ is a constant and τ is the time delay of the reconstruction. In Fig. 1 we plot $n_k(r)$ as a function of r on a log-log scale for increasing embedding dimensions k . We see that the slope of the curves for small distances is constant (corresponding to the one-dimensional attractor of the logistic map) but the curves are shifted by a constant value which indicates the dynamical entropy K_k of the chaotic map.

Due to the positive dynamical entropy, the scales for which the dimension can be resolved go to zero with increasing embedding dimension k . For large distances, the slope becomes arbitrarily large, indicating that iterates of chaotic maps approach stochastic noise. This property is used in the construction of random number generators for computers.

If a system falls onto a low-dimension attractor, the slope

$$D_k \equiv \frac{\log n_k(r)}{\log r} \quad (5)$$

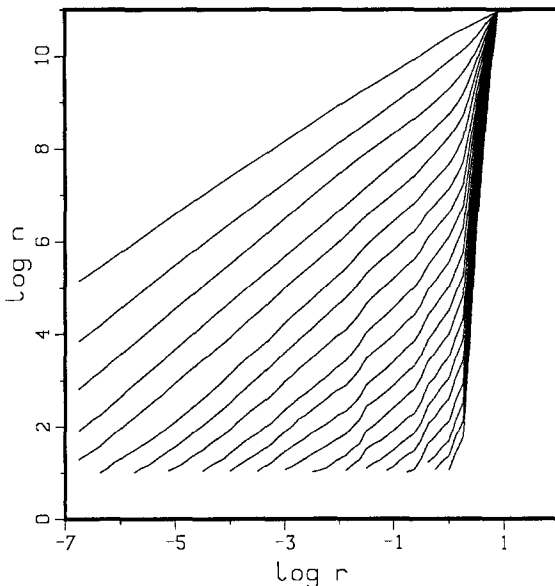


Fig. 1. Number $n_k(r)$ of pairs of vectors (x_i, x_j) within distance r versus separation r on a double logarithmic scale for the one-dimensional single logistic map. [Eq. (2) with $a = 1.95$]. The different curves correspond to increasing embedding dimensions. The slopes of the curves determine the correlation dimension, and their spacing measures their dynamical entropy.

converges to the dimension of the attractor D as k is increased and r goes to zero. In the same way K_k tends asymptotically to the entropy K of the system.

Since we are considering a spatially extended coupled system in which the dimension increases in proportion to the system size, we expect that the dimension D_k observed from a reconstructed time series of a single lattice point will not converge for a given distance r as the embedding dimension k increases. Stochastic noise can be considered as the limit for which the dimension or the entropy becomes infinite. Again this is a mathematical statement and its observability depends on the concrete realization of the system (see, e.g., refs. 27 and 28).

We first discuss the behavior of D_k in a spatially extended system where the $k-d$ dimension D_k does not converge to a constant value within a realistic embedding dimension ($D_k < 20$, say, which is small compared to the total dimension of the full lattice system). If the data are stochastic, $D_k = k$ must hold theoretically. For numerical estimation of this relationship with a limited number of data points (we typically used $n_{\text{data}} = 10^4$ points, but also tested some results with up to $n_{\text{data}} = 3 \times 10^5$), we observe the convex behavior of Fig. 2, which we shall discuss below. In spatiotemporal chaos, where the dynamics is deterministic, the increase of the slope is expected to be smaller than this upper bound given by white noise.

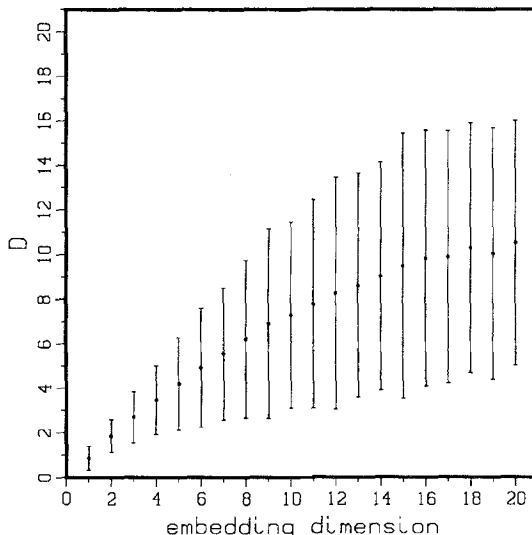


Fig. 2. Observed correlation dimension D_k as a function of embedding dimension k for time series produced by a random generator.

3. LYAPUNOV ANALYSIS AND PROPAGATION OF PERTURBATIONS

In this section we will make an estimate of the increase of the observed dimension as a function of the embedding dimension, using Lyapunov analysis. The main assumption here is that D_k measures the degrees of freedom for the dynamics of k -embedded vectors. We estimate D_k by counting the effective number of degrees of freedom which govern the vector of length k at a fixed lattice point j .

Let us take a one-dimensional lattice system with $j \in [-L, L]$ ($L \geq 50$) and observe the dynamics of the variable x at the point $j=0$. The dynamics of $x(j=0, t)$ is embedded in a k -dimensional phase space by taking $x(j=0, t+1), x(j=0, t+2), \dots, x(j=0, t+k)$. We then ask which lattice points $l \in [-L, L]$ have an influence on the reconstruction of the time-delayed dynamics at $j=0$ for an embedding dimension $k > 1$.

For this purpose, the notion of comoving Lyapunov exponent introduced by R. J. Deissler and K. Kaneko⁽³⁰⁾ is useful. The maximal comoving Lyapunov exponent $\Lambda_1(v)$ is defined as the maximal Lyapunov exponent in the inertial reference frame moving at a constant velocity v relative to the lattice. A small disturbance is then transmitted with the same velocity v by an amplifying (contracting) ratio $\exp[\Lambda_1(v)]$ per unit time. See Fig. 3 for examples of maximum comoving Lyapunov exponents.

If the lattice point l satisfies the condition $\Lambda_1(k/l) > 0$, a small disturbance at the point is transmitted to the point $j=0$ within k steps. Then the

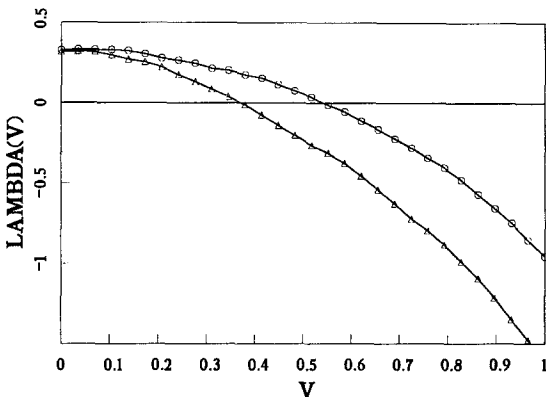


Fig. 3. Maximal comoving Lyapunov exponent for coupled logistic map lattice (\circ) $a = 1.9, \mu = 0.4$; (\triangle) $a = 1.85, \mu = 0.2$) calculated from the product of Jacobi matrices of sub-regions of size of 53 lattice sites for a total lattice of 500 sites. (The Lyapunov exponents were calculated for 2000 steps after 1000 transients.) The condition $\Lambda_1(v_p) = 0$ determines the maximal velocity v_p of propagation for disturbances in the lattice.

dynamics of lattice point l is relevant to determine the k -embedded dynamics at $j=0$. This condition leads to

$$|l| < k v_p \quad (6)$$

where the maximal propagation velocity of perturbations can be determined through $A_1(v_p) = 0$.⁽²⁹⁾ The region which satisfies Eq. (6) can be thought of as an “effective light cone.”

In a spatially extended system, intensive quantifiers such as entropy density are useful. Lyapunov spectra are defined from the product of Jacobi matrices as usual. An example of spectra is shown in Fig. 4.

In direct correspondence to the dimension in dynamical systems, we can define the (Lyapunov) dimension density. The Lyapunov dimension is calculated from the Lyapunov spectra λ_i in a subspace with size M by

$$\rho = \frac{1}{M} \left(j + \frac{\sum_{i=1}^j \lambda_i}{|\lambda_{j+1}|} \right) \quad (7)$$

with j such that $\sum_{i=1}^j \lambda_i > 0$ and $\sum_{i=1}^{j+1} \lambda_i < 0$ ($j+1 \leq M \leq N$). The interpretation of dimension density rests in the fact that each lattice point has effectively ρ degrees of freedom. Metric entropy density κ is calculated in a similar way as

$$\kappa = \frac{1}{M} \sum_{i=1}^j \lambda_i \quad (8)$$

with j such that $\sum_{i=1}^j \lambda_i > 0$ and $\sum_{i=1}^{j+1} \lambda_i < 0$. The above two estimates lead to the upper bound for the effective number of degrees of freedom deter-

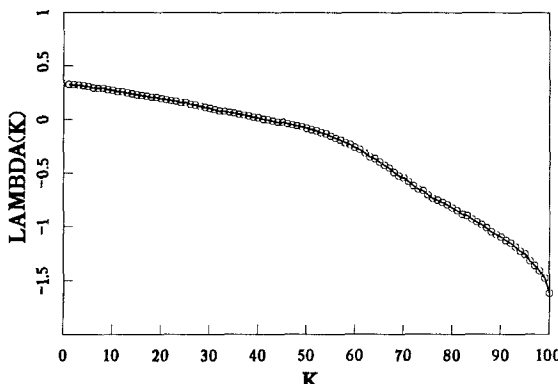


Fig. 4. Lyapunov spectrum for coupled logistic map lattice ($\alpha = 1.9$, $\mu = 0.4$) calculated from the product of Jacobi matrices for 3000 steps after 2000 transients.

mined from orbits embedded in a k -dimensional state space. From these estimates we get an inequality for the estimated dimension D_k :

$$D_k \leq 2\rho v_p k \equiv c_0 k \quad (9)$$

In the above argument, all the regions $|l| < kv_p$ contribute fully to the dynamics of the lattice point at $j=0$, but this is an overestimate. Indeed, if $|l|$ gets larger, the contribution must be smaller, since the comoving Lyapunov exponent decreases with velocity. We can obtain a slightly better bound, as discussed in the next section, by taking account of this effect. The inequality in Eq. (9) comes from the fact that the correlation dimension of low-dimensional dynamical systems typically is smaller than the Lyapunov dimension.

3.1. Effective and Comoving Lyapunov Dimension

First, let us introduce the comoving Lyapunov spectra $\Lambda_i(v)$. This is a straightforward generalization of maximal comoving Lyapunov exponent. Take a large subregion and calculate the long-time product of Jacobi matrices in a comoving frame of velocity v .⁽³⁰⁾ Logarithms of absolute values of eigenvalues divided by time steps give the comoving Lyapunov spectra. The maximal comoving Lyapunov exponent in the previous section is the first exponent $\Lambda_1(v)$. The conventional Lyapunov spectra λ_i are obtained as $\Lambda_i(0)$. Examples of comoving Lyapunov spectra are shown in Fig. 5.

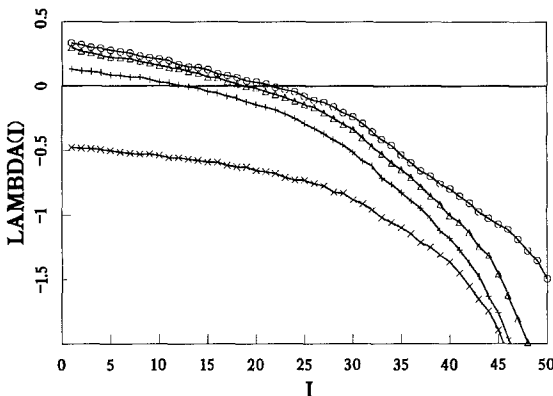


Fig. 5. Comoving Lyapunov spectra for coupled logistic lattice ($a = 1.9, \mu = 0.4$) calculated from the product of Jacobi matrices from a subregion of size 50 of a total lattice of size $N = 500$. The average is taken over 1000 time steps after 1000 transients. Plotted are the spectra for $v = (\circ) 0, (\triangle) 0.1, (+) 0.4, (x) 0.8$.

The comoving Lyapunov dimension density is defined as

$$d_L(v) = \frac{1}{M} \left[j(v) + \frac{\Lambda_1(v) + \cdots + \Lambda_j(v)}{|\Lambda_{j+1}(v)|} \right] \quad (10)$$

with $j(v)$ such that $\sum_{i=1}^{j(v)} \Lambda_i(v) > 0$ and $\sum_{i=1}^{j(v)+1} \Lambda_i(v) < 0$. This quantity is a Lyapunov dimension density in a Galilean frame of reference with velocity v . The comoving Lyapunov dimension density ρ is given by $d_L(0)$ (Fig. 6). The comoving Lyapunov dimension density which describes the influence of a perturbation at a lattice point l on a k -vector at site $j=0$ is given by $d_L(l/k)$. Thus the upper bound for the dimension D_k is estimated by

$$D_k \leq \sum_{l=0}^{d_L(l/k) > 0} d_L(l/k) \equiv ck \quad (11)$$

[summation is taken while $d_L(l/k) > 0$, in other words, $|l| < kv_p$]. Since $d_L(l/k) \leq \rho$, the above estimate gives a better bound than that in the previous section, which is obtained by taking $d_L(l/k) = \rho$. Numerical data for the metric entropy density κ , the Lyapunov dimension density ρ , the maximal propagation velocity v_p , and the increase rates of the $k-d$ Lyapunov dimension c_0 and c for the logistic lattice with nonlinearity parameter a and coupling parameter μ are shown in Table I.

3.2. Estimate of Dimension Density

It is impossible to obtain the dimension density and velocity separately from a reconstruction using a single lattice point. This separation is

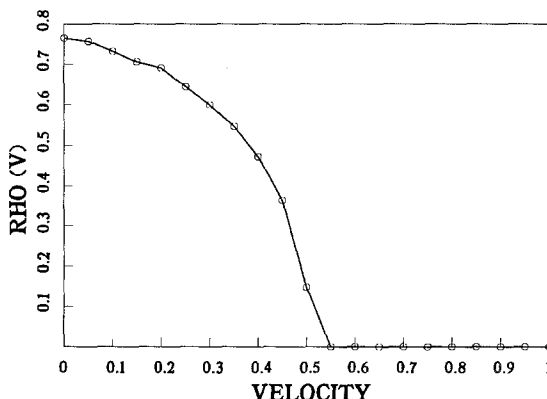


Fig. 6. Comoving Lyapunov dimension density for coupled logistic lattice ($a = 1.9$, $\mu = 0.4$) calculated from the product of Jacobi matrices from a subregion of size 50 of a total lattice of size $N = 5000$. The average is taken over 1000 time steps after 1000 transients.

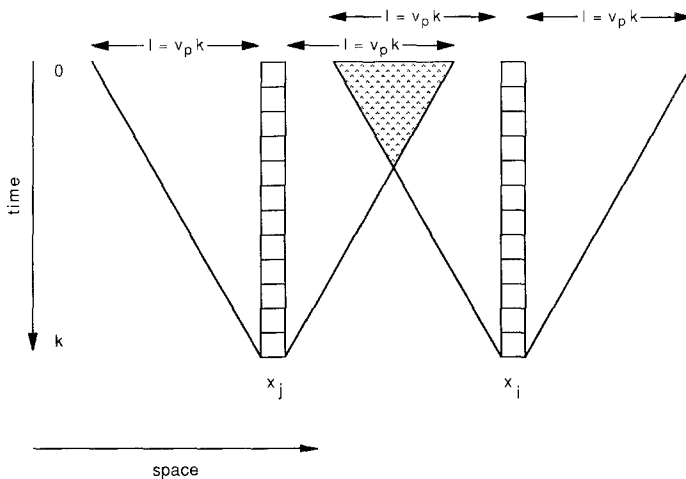


Fig. 7. Two-point measurement of time series x_j and x_i at locations j and i . The shaded regions indicates lattice points from which perturbations will influence both vectors $\mathbf{x}(j, t=0)$ and $\mathbf{x}(i, t=0)$.

possible, however, from an observation and reconstruction using two spatially distant points (for similar ideas see refs. 31 and 34; see also refs. 15 and 33).

Let us denote the distance between the two points a and b as R . First we use the rough argument in Section 2: If the two points are separated by an amount greater than the effective light cone given by the condition

$$R > 2v_p k \quad (12)$$

then the two vectors reconstructed from the two points are effectively independent. Thus, the bound of the observed dimension is just a sum of the dimensions from the two single points, i.e.,

$$D^{(2)}(k; R) < 4\rho v_p k = 2c_0 k \quad (13)$$

On the other hand, if the embedding dimension k is larger than $R/(2v_p)$, the two effective light cones overlap (see Fig. 7). Since the region should be counted only once in the two-point observation, we have to cancel the double counting of the region from the above estimate, which leads to

$$D^{(2)}(k; R) < 2\rho v_p k + R\rho = c_0 k + R\rho \quad (14)$$

If the inequality in the above estimate is not too large, it gives a way to see the velocity and dimension density separately. The above estimate leads to

$$\rho = \frac{1}{R} \left(D^{(2)}(k; R) - \frac{1}{2} (D_{k,a} + D_{k,b}) \right) \quad (15)$$

which in the continuum limit $R \rightarrow 0$ becomes:

$$\rho = \frac{\partial D^{(2)}(k; R)}{\partial R} \quad (16)$$

where slopes $D_{k,a}$ and $D_{k,b}$ obtained by a single point reconstruction at sites a and b take the same value $2\rho v_p k$, since we assume spatial homogeneity.

The above argument can be slightly modified in a manner similar to the analysis of the comoving Lyapunov dimension. The value c_0 should be replaced by c and the transition from the behavior according to Eq. (14) to that of Eq. (15) will be smooth in numerical realizations. The final result (16) does not change for large embedding dimensions, since $d_L(R/k)$ of Eq. (10) approaches ρ for large embedding dimensions k .

4. DIRECT NUMERICAL DIMENSION ESTIMATES

4.1. Delay Time Dependence of D_k

In the estimate of dimension in low-dimensional systems, it has been shown by Takens⁽⁵⁾ that for a generic choice of delay times the geometrical reconstruction method provides an embedding of the attractor which produced the observed time series. For numerical realizations, however, this embedding can be effectively degenerated (e.g., the extension in some coordinate directions can be smaller than the noise resolution) such that for continuous time series the choice of an optimal delay time is important (see, e.g., ref. 27). Furthermore, a positive Kolmogorov–Sinai entropy K induces amplification of low-level perturbations, which in turn increases the observed dimensionality at a given scale for a certain embedding dimension. We observe a similar effect in large, spatially extended systems: Since the observed dimension D_k increases with k , a different delay in the reconstruction corresponds to selecting vectors of the space of the same Euclidean dimension, but the distribution of the components will typically be quite different, as reflected in the finite resolution estimates of the correlation dimension.

The dependence of D_k on the choice of delay time is due to a change of region in the effective light cone. If the delay time is increased by a factor of two, the effective spatial range increases by the same factor, since the time scale for the velocity v_p is reduced by half. Generally, for the system measured by m steps, the term v_p in the above formulas should be replaced by mv_p . This gives a possible simple diagnosis to distinguish random data from spatiotemporal chaos, since in the random data $D_k = k$ holds irrespective of m , if the delay time in the sampling is larger than the correlation time of (colored) noise.

4.2. Correlation versus Lyapunov Dimension

For the calculation of quantities based on Lyapunov exponents we need to know the derivatives of the dynamics of the system, which often poses a severe complication for experimentally obtained time series. Therefore we compare the above results with those directly obtained from reconstructed time series using numerical algorithms for estimating correlation dimensions (for details of the algorithm see ref. 32). As mentioned above, the values obtained from correlation dimension estimates are typically lower than the Lyapunov dimension values. These differences are especially large when the invariant measure of the system has many singularities and therefore a broad $f(\alpha)$ spectrum (see, e.g., ref. 40). We know that the single logistic function has a multifractal measure and we also expect that for the coupled system some of these singular properties will persist (see also the discussion in refs. 27 and 28). Thus, the above estimate of the slope for D_k by Lyapunov dimensions is always an upper bound for the corresponding values obtained from correlation dimensions.

In Table I we present the numerical results for the estimated correlation dimension D_{20} (these values are not calibrated with the noise data) at a single lattice point ($j = 49$) for an embedding of $k = 20$. For these calculations we iterated the complete lattice for $n = 25,000$ iterations to let transient behavior die out and then computed the correlation dimension on a set of the following $n_{\text{data}} = 10,000$ points. The two-point dimension $D_k^{(2)}$ is obtained by intertwining time series obtained from two lattice points i, j separated by a distance $\Delta = |i - j|$ (see refs. 33 and 34). For most parameter combinations we see only a very slight increase in the two-point dimension compared to the single-point dimension, which corresponds to a very low dimension density $\rho_d = (1/\Delta)(D_k^{(2)} - D_k)$, where in our cases we have $k = 20$ and typically $\Delta = 2$. The only exceptions seem to be the cases with low non-linearity a and high coupling μ , where the results differ from those obtained

Table I. Quantification of Spatiotemporal Chaos in Coupled Map Lattices

a	μ	κ	ρ	v_p	c_0	c	D_{20}	$d_{20}^{(2)}$	c_d
1.95	0.4	0.084	0.77	0.55	0.86	0.61	4.3	4.9	0.34
1.90	0.4	0.074	0.74	0.54	0.80	0.56	4.0	4.4	0.30
1.85	0.4	0.067	0.72	0.53	0.76	0.53	3.8	4.2	0.16
1.80	0.4	0.053	0.67	0.48	0.65	0.48	3.2	4.5	0.10
1.95	0.2	0.16	1.0 ^a	0.40	0.8	0.54	4.3	4.7	0.26
1.85	0.2	0.12	1.0 ^a	0.37	0.74	0.49	4.0	4.4	0.24

^aSince the logistic map is not invertible, the Lyapunov dimension can be larger than the embedding dimension.

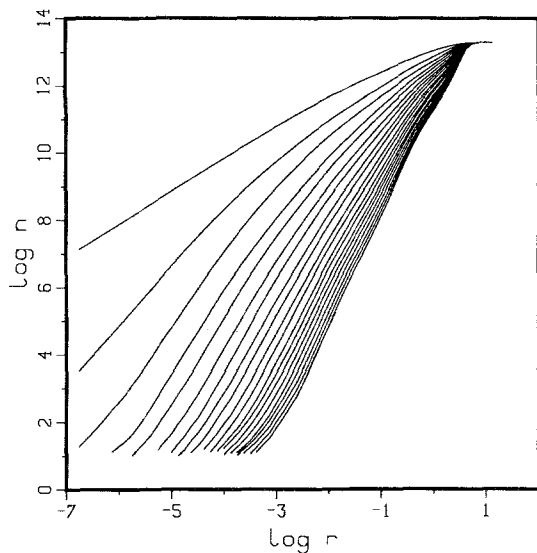


Fig. 8. Correlation integral $n_k(r)$ [see Eq. (4)] for time series $x(i=49, t)$ of the logistic lattice [Eq. (1)] of size $N = 100$ and $a = 1.8$, $\mu = 0.4$. The calculations were performed on $n_{\text{data}} = 10^4$ points after $n_{\text{trans}} = 2 \times 10^4$ transients. The time delay in the reconstruction is $\tau = 1$ and the embedding dimensions were $k = 1, \dots, 20$.

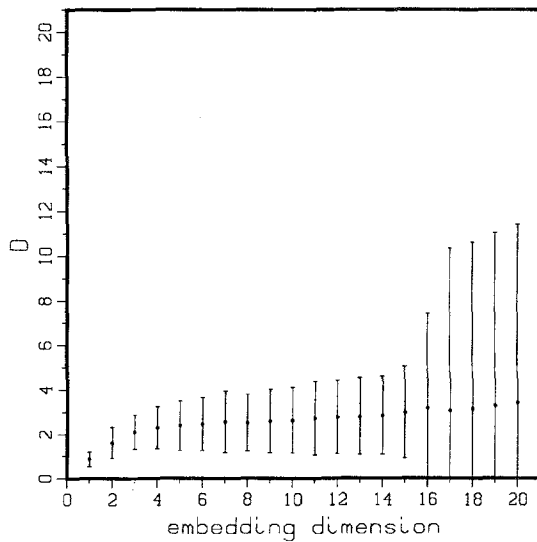


Fig. 9. Same as in Fig. 2 for the data of Fig. 8.

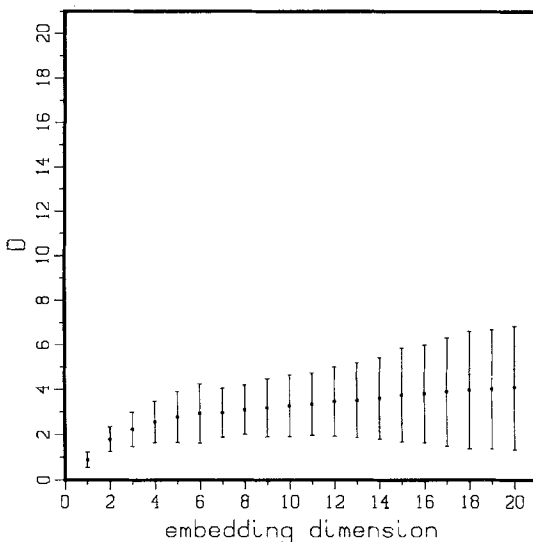


Fig. 10. Same as in Fig. 9 for data from two-point time series $[x(i=49, t), x(i=52, t)]$ with the same parameters as in Fig. 8.

from Lyapunov estimates. Finally, we estimated the increase rate c_d (normalized with respect to the noise data of Fig. 2) of the observed dimension with the embedding dimension. These results show a dependence on the parameters a and μ which is in good agreement with the corresponding values for c_0 and c obtained from the Lyapunov analysis.

Some of the geometrical and statistical factors which decrease the numerically observed values for the correlation dimension are discussed in refs. 27, 28, and 32). It is therefore very difficult to estimate accurately the absolute values of dimensions in situations where the dynamics is very complex. A method introduced by Somorjai⁽³⁵⁾ calibrates the numerical results with respect to the "white noise" signal obtained from the numerical random number generators (see Fig. 2). This is especially relevant if the system is very noisy in the sense that the observed dimension D_k increases rapidly with k , i.e., the above rate c is close to 1. This effect is even more pronounced in the two-point measurement, where the slope is increased drastically. A further complication of the one-dimensional logistic map is its noninvertibility, which also leads to the inapplicability of a Lyapunov dimension formula, e.g., for small coupling μ in combination with large nonlinearity a the dimension density becomes larger than physically reasonable³ and one would have to replace the logistic dynamics by the

³ $c > 1$, and for these cases we cannot use our methods to distinguish a coupled map lattice from stochastic noise. A similar situation occurs for lattices in higher dimensions.

invertible dynamics of its extension, the two-dimensional Hénon map. In a future study we plan to extend our investigations to coupled Hénon map lattices which would be equivalent to systems of coupled and driven oscillators with finite damping (note that the logistic map corresponds to the limit of infinite damping).

5. LATTICES IN HIGHER SPATIAL DIMENSIONS

We can simply extend the argument to spatiotemporal chaos in a higher spatial dimension. For a single slope this is estimated by

$$D_k \leq \text{const} \times \rho(v_p k)^d \quad (17)$$

for a d -dimensional lattice system. If $d > 1$, the above estimate ultimately exceeds the upper bound $D_k = k$, as the embedding dimension gets larger. We may observe a crossover from k^d to linear behavior. This means that within a single-point reconstruction, it is impossible to distinguish spatiotemporal chaos from random data. We may extend a two-point observation in Section 4 to a multipoint, or to a measurement at points on a curve or sphere, but this looks practically impossible due to the limitations of the computational abilities available today.

6. NOISE-INDUCED TRANSITIONS

In the previous sections we treated the coupled lattice of logistic maps as a noise simulator and have therefore chosen the system parameters so that the dynamics on the lattice was uniformly chaotic. We have seen that additional noise has only minor effects on the lattice dynamics. In the following we discuss briefly the interaction of the lattice dynamics with external noise. We have changed the parameters to $a = 1.7$ and $\mu = 0.4$, so that the chaotic dynamics is now confined to bounded domains which are separated by regions of periodic dynamics.⁽³⁶⁾ The pattern of chaotic and periodic regions depends strongly on the initial conditions. Thus, the question arises of whether this pattern selection mechanism is due to coexisting spatiotemporal attractors.

In Fig. 11a we have a state with five primary cells exhibiting chaotic behavior. The system is deterministic (i.e., noise level $\sigma = 0$) and the initial conditions are taken as a fixed random sequence. The boundary conditions are periodic. In Fig. 11b we see the influence of external, uniform, and bounded perturbations ($\sigma = 0.005$). The state of Fig. 11a is reproduced

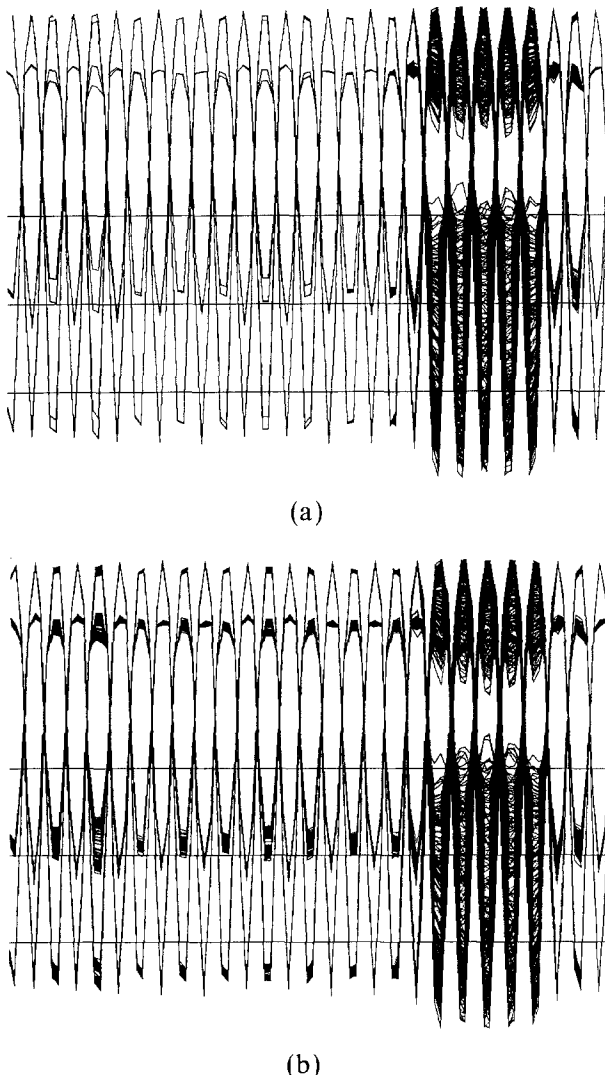
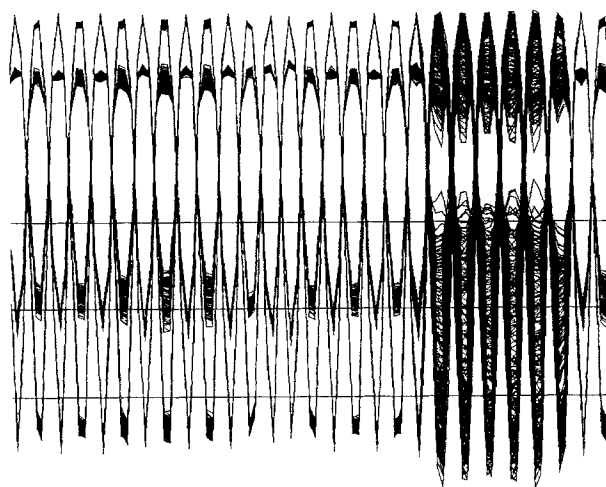
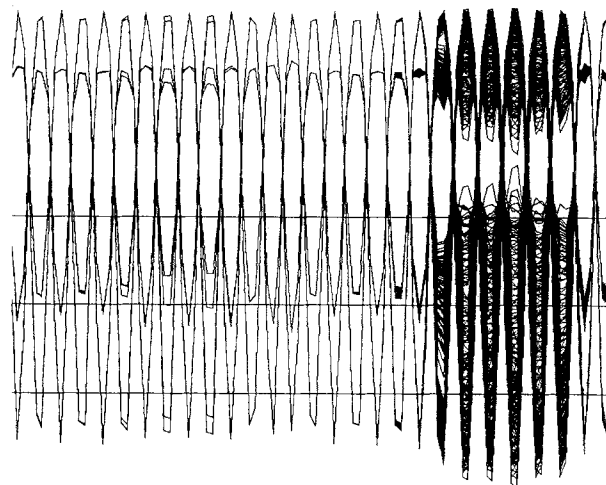


Fig. 11. (a) Superposition of 500 iterates of the coupled map lattice (vertical axis) of Eq. (1) for the parameters $a = 1.7$ and $\mu = 0.4$ versus lattice position (horizontal axis). Superimposed on the primary periodic structure (cells) there exists a chaotic domain extending over five primary cells. Initial values are random. (b) Same as in (a) but with the addition of uniformly distributed, delta-correlated random fluctuations with bounded amplitude ($\sigma = 0.005$). The spatial structure is still preserved. (c) Same as in (a) but with a noise level of $\sigma = 0.01$. Now the spatial structure consists of six chaotic cells, a new attractor which was generated through a noise-induced transition. (d) Same as in (a), but as initial conditions we chose the final state of (c). The noisy perturbations in the regular part of the lattice have disappeared and the structure of the attractor is apparent.



(c)



(d)

Fig. 11 (*continued*)

when the noisy perturbations are removed. This clearly indicates the attractive nature of the spatial pattern on the lattice. For a larger noise level ($\sigma = 0.01$), we observe a transition to a new state with a chaotic domain of six primary cells. This new state appears to be more robust against external noise perturbations than the five-cell state of Fig. 11a, since it returns to the deterministic attractor of Fig. 11d when the noise is removed. This observed asymmetry of noise-induced transitions between coexisting attractors has been previously observed in the context of smooth perturbations of the logistic map on the interval which has coexisting attractors in regions with positive Schwarzian derivative.⁽³⁷⁾ There it also has been demonstrated that the statistical nature of the perturbation (e.g., noise versus periodic) is extremely relevant for the kinds of transitions which can occur. The theory of these nonlinear resonance effects has been developed and generalized by Hübler and Lüscher,⁽³⁸⁾ and it turns out to be very successful in controlling chaotic dynamics. In a forthcoming paper we discuss in more detail pattern selection processes which are related to external perturbations.⁽³⁹⁾

One interpretation of this state of the system is that we have multistability in the sense of coexistence of several attractors for the same parameter combination. In order to test this hypothesis, we perturbed the system with additive, finite-amplitude delta-correlated noise. For the case that the domains are mere reflections of the initial state we expect that small, random perturbations will destroy the domains in a random walk process. In the case of stable attractors, however, we expect that random perturbations will not strongly alter the solution. Furthermore, the system should return to its original state when the noise source is removed.

ACKNOWLEDGMENTS

The authors would like to thank James Crutchfield, Doyne Farmer, Masaki Sano, Norman Packard, Yoshitsugu Oono, Th. Kurz, and David Umberger for useful discussions, and B. Ecke for carefully reading the manuscript. One of the authors (K.K.) would also like to thank his colleagues at the CNLS at Los Alamos and the CCSR at the University of Illinois at Urbana-Champaign for their hospitality during his stay. He thanks the Ministry of Education, Japan, for financial support for his stay at Illinois.

REFERENCES

1. A. J. Lichtenberg and M. A. Lieberman, *Regular and Stochastic Motion* (Springer, Berlin, 1983); P. Berge, Y. Pomeau, and C. Vidal, *L'Ordre dans le Chaos* (Hermann, Paris 1984);

- H. G. Schuster, *Deterministic Chaos* (Physik Verlag, Weinheim, 1984); H. Haken, *Advanced Synergetics*, (Springer, Berlin, 1983).
2. G. J. Chaitin, *Sci. Am.* **1975** (May):47.
 3. A. N. Kolmogoroff, *Prob. Inf. Transmission* **1**:3 (1965).
 4. N. H. Packard, J. P. Crutchfield, J. D. Farmer, and R. S. Shaw, *Phys. Rev. Lett.* **45**:712 (1980).
 5. F. Takens, *Lect. Notes Math.* **898**:366 (1981).
 6. J. D. Farmer, E. Ott, and J. A. Yorke, *Physica* **7D**:153 (1983).
 7. G. Mayer-Kress, ed., *Dimensions and Entropies in Chaotic Systems—Quantification of Complex Behavior* (Springer-Verlag, Berlin, 1986).
 8. K. Kaneko, *Collapse of Tori and Genesis of Chaos in Dissipative Systems* (World Scientific, Singapore, 1986).
 9. J. P. Crutchfield and K. Kaneko, in *Directions in Chaos* (World Scientific, Singapore, 1987).
 10. Y. Oono and S. Puri, *Phys. Rev. Lett.* **58**:836 (1986).
 11. H. Chate and P. Manneville, *Physica D*, to appear, and preprint.
 12. S. Wolfram, *Theory and Applications of Cellular Automata* (World Scientific, Singapore, 1986).
 13. J. P. Crutchfield, Ph. D. Thesis, University of California, Santa Cruz (1983).
 14. R. J. Deissler, *Phys. Lett.* **100A**:451 (1984).
 15. K. Kaneko, in *Dynamical Systems and Singular Phenomena*, G. Ikegami (World Scientific, Singapore, 1987).
 16. J. P. Crutchfield and K. Kaneko, in preparation.
 17. P. Grassberger, Information content and predictability in lumped and distributed dynamical systems, Preprint Wuppertal WB 87-8.
 18. I. Waller and R. Kapral, *Phys. Rev.* **30A**:2047 (1984); R. Kapral, *Phys. Rev.* **31A**:3868 (1985).
 19. K. Kaneko, *Prog. Theor. Phys.* **72**:480 (1984); **74**:1033 (1985).
 20. T. Yamada and H. Fujisaka, *Prog. Theor. Phys.* **72**:885 (1985).
 21. J. D. Keeler and J. D. Farmer, *Physica* **23D**:413 (1986).
 22. F. Kaspar and H. G. Schuster, *Phys. Lett.* **113A**:451 (1986); F. Kaspar and H. G. Schuster, *Phys. Rev. A* **36**:842 (1987).
 23. T. Bohr, G. Grinstein, Y. He, and C. Jayaprakash, *Phys. Rev. Lett.* **58**:2155 (1987).
 24. P. Alstrom and R. K. Ritala, *Phys. Rev. A* **35**:300 (1987); C. Tang, K. Wiesenfeld, P. Bak, S. Coppersmith, and P. Littlewood, *Phys. Rev. Lett.* **58**:1161 (1987).
 25. P. Grassberger and I. Procaccia, *Phys. Rev. Lett.* **50**:346 (1983).
 26. P. Grassberger and I. Procaccia, *Physica* **9D**:189 (1983).
 27. G. Mayer-Kress, in *Directions in Chaos*, Hao Bai-lin, (World Scientific, Singapore, 1987).
 28. J. Theiler, Quantifying chaos: Practical estimation of the correlation dimension, Ph. D. thesis, California Institute of Technology (1987).
 29. K. Kaneko, *Physica* **23D**:436 (1986).
 30. R. J. Deissler and K. Kaneko, *Phys. Lett.* **119A**:397 (1987).
 31. K. Kaneko, Talk, Meeting of the Physical Society of Japan (1986), unpublished; J. P. Crutchfield, Talk, Pecos Conference on Dimension and Entropy (1985).
 32. J. Holzfuss and G. Mayer-Kress, in *Dimensions and Entropies in Chaotic Systems—Quantification of Complex Behavior*, G. Mayer-Kress, ed. (Springer-Verlag, Berlin, 1986).
 33. G. Mayer-Kress and Th. Kurz, *J. Complex Syst.* **1**:821–829 (1987).
 34. Y. Pomeau, *C. R. Acad. Sci. Paris* **300** (Ser. II, 7):239 (1985).
 35. R. L. Somorjai, in *Dimensions and Entropies in Chaotic Systems—Quantification of Complex Behavior*, G. Mayer-Kress, ed. (Springer-Verlag, Berlin, 1986).

36. K. Kaneko, *Phys. Lett.* **125A**:31 (1987); *Eur. Phys. Lett.* **6**:193 (1987); *Physica D*, to appear.
37. G. Mayer-Kress and H. Haken, *Physica* **10D**:329–339 (1984).
38. A. Hübler and E. Lüscher, Resonant stimulation and control of nonlinear oscillators, Preprint, Stuttgart (1988).
39. V. English and G. Mayer-Kress, in preparation.
40. I. Procaccia, in *Dimensions and Entropies in Chaotic Systems—Quantification of Complex Behavior*, G. Mayer-Kress, ed. (Springer-Verlag, Berlin, 1986).